ScientificScholar®
Knowledge is power
Publisher of Scientific Journals

www.clinicalimagingscience.org

Journal of Clinical Imaging Science

Pictorial Essay

Magnetic Resonance Imaging of the Diaphragm: From Normal to Pathologic Findings

Giuseppe Cicero, Silvio Mazziotti, Alfredo Blandino, Francesca Granata, Michele Gaeta

Section of Radiological Sciences, Department of Biomedical Sciences and Morphological and Functional Imaging, University of Messina, Messina, Italy.

***Corresponding author:**
Giuseppe Cicero, MD, Section of Radiological Sciences, Department of Biomedical Sciences and Morphological and Functional Imaging, University of Messina, Messina, Italy.

gcicero@unime.it

Received : 07 December 19
Accepted : 17 December 19
Published : 13 January 20

DOI
10.25259/JCIS_138_2019

Videos available on:
www.clinicalimagingscience.org
Quick Response Code:

ABSTRACT

The diaphragm is a musculotendinous structure that divides the chest from the abdomen. Its motility, unintentional or voluntary, is crucial for the physiologic respiratory function due to its contribution to lung volume expansion and contraction. Therefore, diaphragmatic dysfunction may cause a respiratory failure without any pathology of the lungs. Different imaging modalities can be employed for diaphragmatic evaluation. Among all, magnetic resonance imaging (MRI) has demonstrated to be the most accurate technique in providing a morphologic and functional assessment of the diaphragm as well as information about the adjacent structures. However, its diagnostic value is still underrated and its performance is often far from the daily clinical practice. Backward, physicians and radiologists should be aware of the undoubted advantages of MRI and confident about the normal or pathologic imaging features, to avoid misdiagnosis.

Keywords: Magnetic resonance imaging, Diaphragm, Diaphragmatic diseases

INTRODUCTION

The diaphragm is a dome-shaped musculotendinous structure placed between the thorax and the abdominal cavity.

It is considered the main inspiratory muscle, since its contraction causes the enlargement of the chest with consequent pressure lowering and airways gas filling.

Backward, its relaxation increases the thoracic pressure enabling expiration.[1,2]

Different imaging modalities can be employed for the evaluation of the diaphragm. X-ray plain film still represents the initial imaging step for diaphragmatic pathology, although it can only provide a few morphologic information.[1,3]

Computed tomography (CT)-scan can provide morphological but not functional information about the diaphragm.

On the other hand, conventional fluoroscopy, ultrasound (US), and magnetic resonance (MR) are able to overcome the mere morphologic assessment, extending the evaluation to the diaphragmatic functionality, through a real-time appraisal.[3-5]

Compared to fluoroscopy, the US comes with the advantages of lack of radiation exposure, easy portability, and capability of both morphologic and functional assessment. The main findings quantifiable on the US are diaphragmatic thickness and amplitude of excursion during free or forced breathing.

Figure 1: Normal diaphragmatic magnetic resonance imaging findings. Coronal (a) and axial (b) turbo spin echo T2-w sequences showing the normal morphology and hypointensity of the diaphragm (arrowheads) and diaphragmatic crura (arrows). Sagittal balanced-fast field echo scans performed at full inspiration (c) and full expiration (d) demonstrate the physiologic diaphragmatic excursion. Asterisks: Iliopsoas muscles.

However, US limitations consist in the restricted field of view, the possible impairment of lung air or bowel gas superimposition, and the strictly reliance on the operator's expertise.[3,4]

As well as the US, MR imaging (MRI) is a radiation-free technique that can provide a static or dynamic evaluation with the further benefit of a wider field of view and a more detailed soft tissue characterization.[4]

In particular, the latter considerations are particularly important in the challenging differential diagnosis of lung diseases from diaphragm weakness in patients suffering from respiratory failure.[6]

Beyond the limits of a time-consuming exam and the indispensable patient's compliance, MRI is currently the most comprehensive imaging modality in the evaluation of diaphragmatic pathologies.

Hence, the aim of this paper is to provide an overview of normal and pathological features of the diaphragm on MRI and, therefore, to demonstrate the usefulness of this technique in different clinical circumstances.

CLINICAL APPLICATIONS

Normal MRI findings

The diaphragm is composed of a central tendon and a peripheral muscular component, both provided of three major openings that allow the passage of vascular (caval and aortic hiatuses) and gastroenteric (esophageal hiatus) structures.

The diaphragm is anterolaterally connected to the sternum, the xiphoid process, and to the last six costal cartilages through muscle bundles (or "diaphragmatic slips"), while posteriorly it is attached to the first lumbar vertebral bodies through two musculotendinous structures (the "crura").[1,6]

Innervation is provided by the phrenic nerves, originating from nerve roots C3–C5.[6]

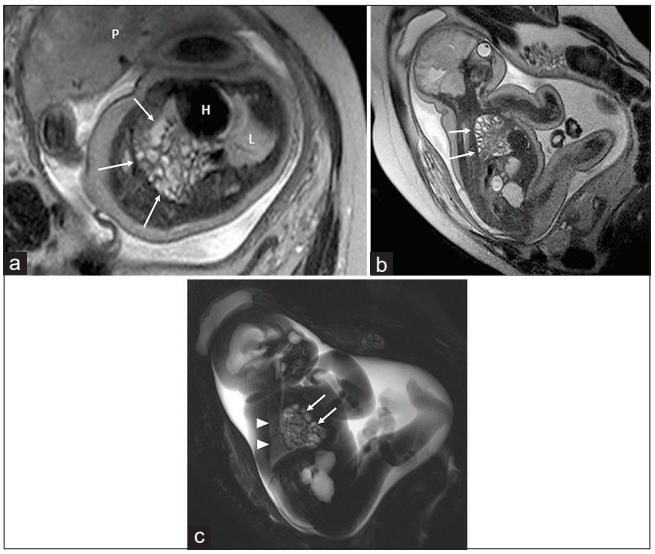

Figure 2: Fetal magnetic resonance imaging in a 32 gestational week fetus. Oblique axial (a) and oblique sagittal turbo spin echo T2-w (b) and oblique sagittal RARE (c) T2-w sequences showing massive transdiaphragmatic herniation of intestinal loops (arrows) with complete replacement of the right lung within the chest. The left lung (L) is normally developed and positioned (arrowheads). P: Placenta. H: Heart.

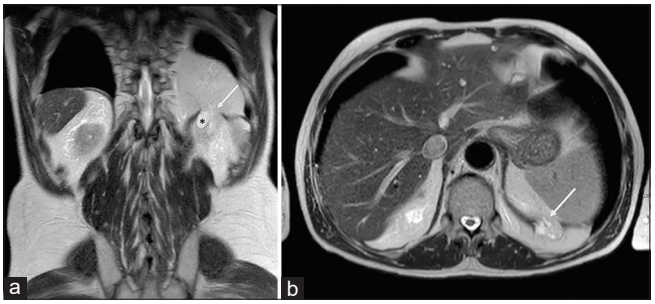

Figure 3: A 74-year-old male patient. Coronal (a) and axial (b) T2-w turbo spin echo acquisitions demonstrated, as an incidental finding, an abruption of the left hemidiaphragm (arrow) with mesenteric fat herniation and partial involvement of a left kidney simple cyst (asterisk).

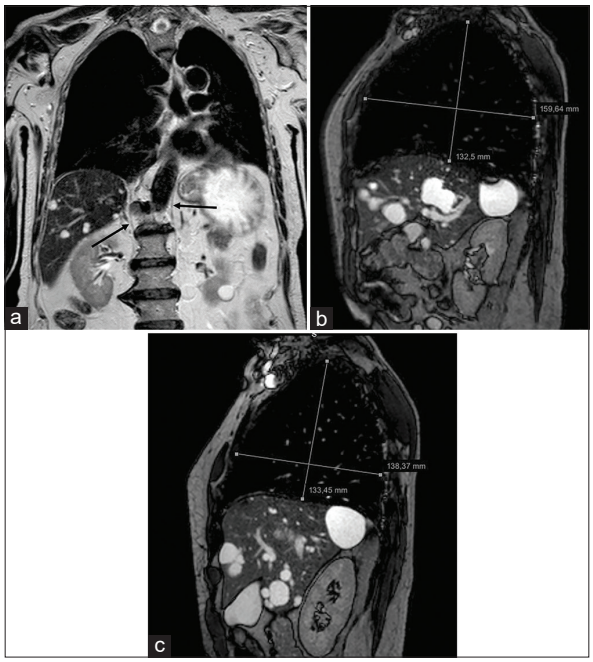

Figure 4: A 76-year-old male patient affected by Pompe disease. Coronal turbo spin echo T2-w acquisition (a) shows and advanced state of hypotrophy of both the diaphragmatic crura (arrows). Sagittal balanced-fast field echo scans, performed at end-inspiration (b) and end-expiration (c), demonstrate a slight lung volume change, mainly appreciable on the anteroposterior plane, due to both the decreased function of the diaphragm and the partial intercostal muscles compensation.

Normally the diaphragm looks like a thin band with low signal intensity on both the T1-w and T2-w images.[3]

Beyond the morphologic and structural assessment, the use of dynamic gradient echo recalled acquisitions for the evaluation of diaphragmatic excursion has been longstanding established.

This type of sequences enables to obtain sequential images that can be acquired on the coronal or sagittal planes during real-time breathing. Afterward, the images can be displayed in a cine-loop viewing, thus providing a dynamic report about diaphragmatic motion.[7]

MRI overcomes the achievements of conventional fluoroscopy and US, thanks to its safeness and the wide field of view [Figure 1 and Video 1].

DIAPHRAGMATIC DEFECTS

Congenital hernias

Congenital diaphragmatic hernias are determined by an incomplete fusion of the pleuroperitoneal membranes and/or the embryologic mesodermal elements of the diaphragm.[8,9]

The usual classification includes: Intrapleural (or Bochdalek), mediastinal (or Morgagni), and hiatal herniations: The formers mainly cause lung hypoplasia and mediastinal shift to the contralateral side due to the thoracic herniation of abdominal content; mediastinal hernias occur posteriorly to

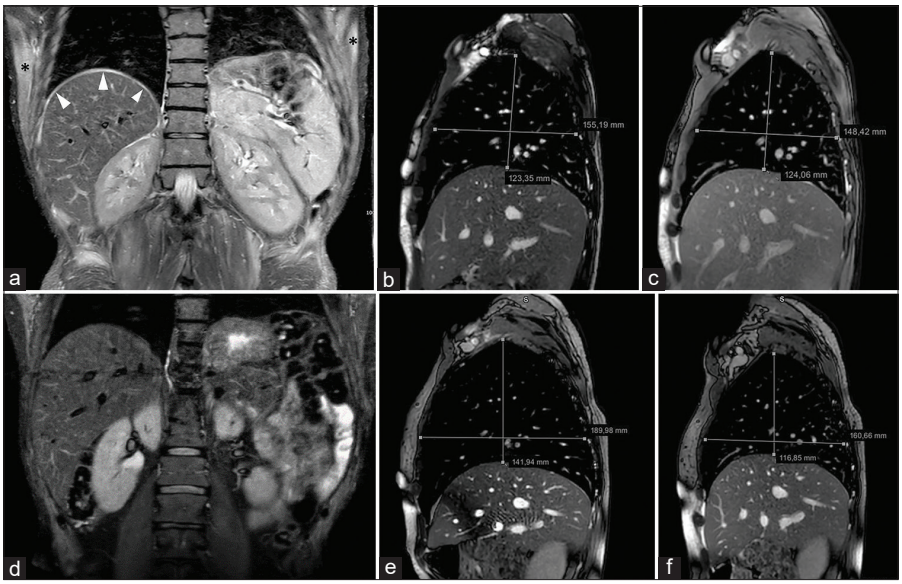

Figure 5: A 45-year-old male complaining lower limb pain and weakness as well as shortening of the breath. Magnetic resonance imaging demonstrated polymyositis. Coronal fast T2-w STIR scan (a) shows hyperintensity of the right hemidiaphragmatic dome (arrowheads) and upper position of the left diaphragm due to inflammation. Note the presence of a bilateral hyperintensity of the chest wall muscles (asterisks). Sagittal balanced-fast field echo scans (acquisition time: 0.6 s) passing through the middle of the right diaphragm, acquired in deep inspiration (b) and deep expiration (c), demonstrate complete absence of diaphragmatic movement. Coronal T2-w STIR performed 3 months after corticosteroid treatment (d) shows the disappearance of the diaphragmatic and chest muscle edema. On sagittal balanced-fast field echo scans obtained during inspiration (e) and expiration (f), a partial recovery of the movement can be detected. The patient had a significative, although partial, improvement of the respiratory symptoms.

the sternum, with the involvement of liver and bowel, and are mainly related to cardiac malformations; hiatal hernias arise posteriorly within the mediastinum, usually together with esophageal alterations.[1,9]

The first imaging approach is based on endouterine US.[10]

However, when positive, the US is usually followed by MRI for a more accurate assessment in terms of fetal lung volume, organ herniation, and neonatal survival prediction [Figure 2].[10]

Acquired hernias

Traumatic

The injuries of the diaphragm are a relatively rare occurrence in subjects suffering from thoracic-abdominal trauma (0.8–8%) and can be related to blunt or penetrating traumas.

Within the formers, the left hemidiaphragm has demonstrated to be the most vulnerable, due to the lack of liver protection and the inherent structural weakness.[8,11]

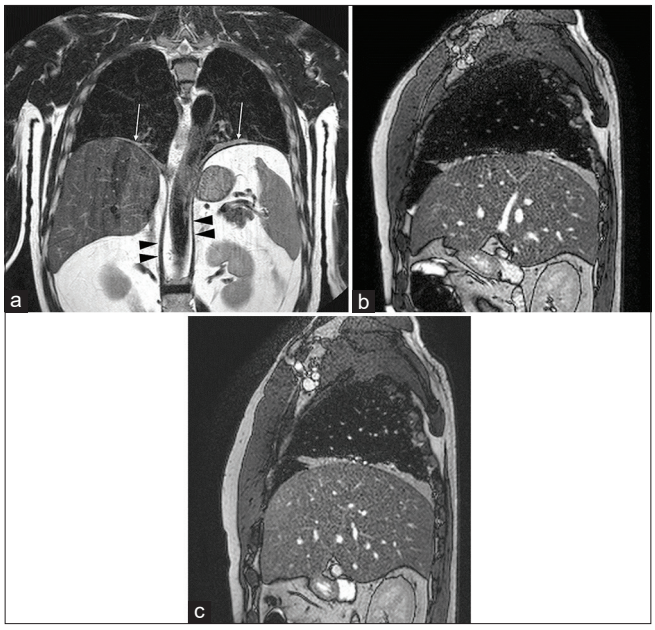

Figure 6: A 50-year-old male patient with respiratory failure of unknown origin. Computed tomography-scan showed bilateral basal bands of parenchymal atelectasis. The functional examination was suspicious for conduction abnormalities of both the phrenic nerves. Coronal turbo spin echo T2-w image (a) shows normal diaphragmatic crura (arrowheads), upper position of both the hemidiaphragms and disventilatory lung parenchyma atelectasis (arrows). Inspiratory (b) and expiratory (c) sagittal balanced-fast field echo scans demonstrate the absence of diaphragmatic movements, a slight increase of the anteroposterior diameter of the lung can be seen during inspiration due to the contraction of the intercostal muscles. The final diagnosis was bilateral phrenic nerve paralysis due to polyneuritis.

Non-traumatic

Acquired hiatal hernias in the adult population are caused by an enlargement of the esophageal hiatus in conjunction with the weakness of phrenoesophageal ligaments.[8]

Diaphragmatic anterior or posterior congenital defects account for some cases of herniation.

Additional conditions, such as increased intra-abdominal pressure due to obesity, can further facilitate their onset.

At MRI, these types of hernias are usually detected as incidental findings [Figure 3].

Weakness and paralysis

Temporary or permanent, unilateral or bilateral diaphragmatic functional deficiencies can arise at three levels: The nervous system, the muscle, or the neuromuscular junction.[2]

The causes are several, from injuries to infections, tumors, inherited metabolic, or collagenous diseases.[2]

As a result, weakness or paralysis with impaired excursion and cranial dislocation of the diaphragm can be detected, with consequent lung parenchyma atelectasis and respiratory distress.

A "real-time" imaging of diaphragmatic function can be performed through fluoroscopy, US, and MRI during normal respiration, deep breathing, or sniffing.

Fluoroscopy allows a two-dimensional evaluation mainly focused on the assessment of the anterior central tendon movements, although with the limit of radiation exposure.[1,4,8]

US focuses more on the posterior and lateral muscular components of the diaphragm and can assess excursion, muscular velocity, and trophism.[3,8]

MRI can rely on fast acquisitions that provide both visual and, through post-processing analysis, quantitative information about diaphragmatic kinetics.[12,13]

Nevertheless, additional sequences can be acquired in all three planes, allowing at the same time lesion characterization and surrounding body tissue evaluation [Figures 4-7 and Videos 2 and 3].[3,6]

Tumors

The diaphragm can be affected by a plethora of benign or malignant primary tumors.

While benign lesions are usually simple cysts (with bronchogenic or mesothelial origin), the most common benign solid tumor is lipoma that, extremely rarely, can show a malignant evolution into liposarcoma.[8,14]

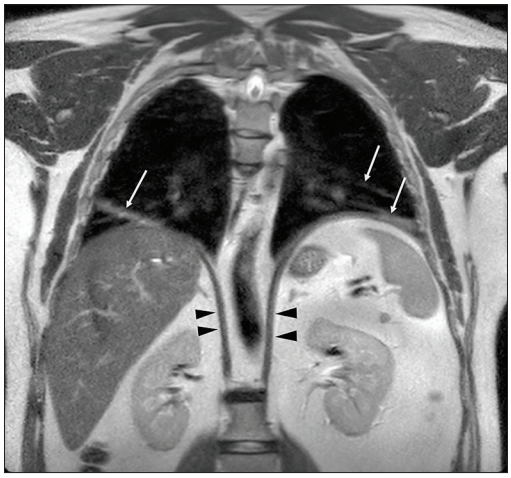

Figure 7: A 53-year-old man presenting with respiratory failure (2% saturation at the rest). Pulmonary disease was suspected, but only basal bands of atelectasis were detected at computed tomography-scan. Coronal turbo spin echo T2-w scan depicts normal diaphragmatic crura (arrowheads), but the anomalous upper position of both the hemidiaphragms and bilateral band of lung atelectasis (arrows). Fluoroscopy magnetic resonance imaging [Video 3] demonstrates severe reduction of the diaphragmatic movements due to weakness. The final diagnosis was myasthenia presenting with respiratory failure.

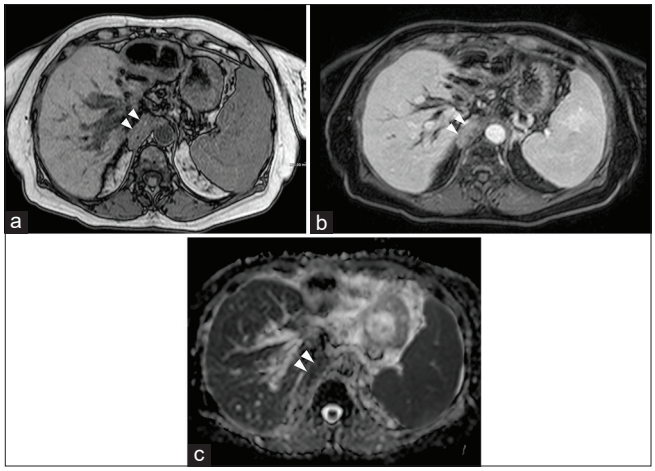

Figure 8: A 64-year-old female patient affected by cholangiocarcinoma. Axial FFE out-of-phase (a) shows the neoplastic involvement of the right diaphragmatic crura (arrowheads). Axial GE T1-w with fat-suppression after the injection of intravenous contrast medium (b) demonstrates an inhomogeneous enhancement, while apparent diffusion coefficient map (c) reveals low values consistent with a high cellular density lesion.

Benign entities are usually asymptomatic unless their size leads to a "mass-effect," generally with respiratory impairment.[8]

On the other hand, rhabdomyosarcoma and leiomyosarcoma are the most frequent cancers, both characterized by poor prognosis.[14]

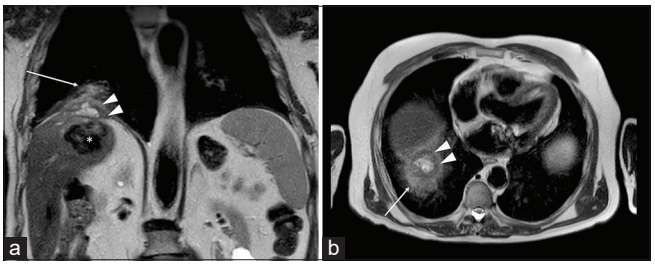

Figure 9: A 71-year-old male patient referred to our hospital for magnetic resonance imaging characterization of a hepatic mass found at ultrasound. Coronal (a) and axial (b) turbo spin echo T2-w scans led to recognize a calcified hydatid cyst within the liver (asterisk) with a cranial extend into the diaphragm, in which well-circumscribed fluid collections, consistent with daughter hydatid cysts (arrowheads) are detectable. Atelectasis of the surrounding lung parenchyma (arrow) is also visible.

Moreover, the diaphragm can be affected by metastasis from primary tumors, especially breast, ovarian, and thymus, or it can be infiltrated by tumors arising in the adjacent, thoracic, or abdominal structures [Figure 8].[1,8,14]

Cystic echinococcosis

Cystic echinococcosis (or "hydatid disease") is considered a separate chapter in the field of cystic lesions. It is generally defined as a zoonotic infection caused by the incidental ingestion of the eggs of a small tapeworm parasite (*Echinococcus granulosus*), and the involvement of the diaphragm is of rare occurrence.

The most common scenario, due to contiguity, consists of the direct extent from the liver (0.6–16%).

Seldom, the diaphragm can be the primary and only site of the implant of the hydatid cysts (1%), through a vascular or lymphatic spread from the bowel.

From this site, the infection can easily diffuse into the thorax, involving mediastinum, pleura, and lung parenchyma with the formation of a bronchial fistula.

MRI has demonstrated to be particularly accurate in the detection and characterization of the fluid and solid components of the cysts [Figure 9].[15-17]

CONCLUSION

The correct diagnosis of diaphragmatic pathologies can be challenging, especially in the context of an accurate differentiation from respiratory diseases.

Due to the wider availability, CT-scan is generally the first-line imaging study, especially in emergency situations, while the US represents a staple approach for a functional assessment.

Beyond the well-known limitations, MRI is currently the technique that best combines the advantages of CT and US, succeeding in providing the most comprehensive evaluation of the main inspiratory muscle.

Therefore, radiologists and physicians should be aware of the diagnostic possibilities of this safe and valuable technique and confident with the images achievable.

Declaration of patient consent

The authors certify that they have obtained all appropriate patient consent forms.

Financial support and sponsorship

Nil.

Conflicts of interest

There are no conflicts of interest.

REFERENCES

1. Abbey-Mensah GN, Waite S, Reede D, Hassani C, Legasto A. Diaphragm appearance: A clue to the diagnosis of pulmonary and extrapulmonary pathology. Curr Probl Diagn Radiol 2017;46:47-62.
2. McCool FD, Manzoor K, Minami T. Disorders of the diaphragm. Clin Chest Med 2018;39:345-60.
3. Chavhan GB, Babyn PS, Cohen RA, Langer JC. Multimodality imaging of the pediatric diaphragm: Anatomy and pathologic conditions. Radiographics 2010;30:1797-817.
4. Kharma N. Dysfunction of the diaphragm: Imaging as a diagnostic tool. Curr Opin Pulm Med 2013;19:394-8.
5. Papa GF, Pellegrino GM, Di Marco F, Imeri G, Brochard L, Goligher E, *et al*. A review of the ultrasound assessment of diaphragmatic function in clinical practice. Respiration 2016;91:403-11.
6. Nason LK, Walker CM, McNeeley MF, Burivong W, Fligner CL, Godwin JD. Imaging of the diaphragm: Anatomy and function. Radiographics 2012;32:E51-70.
7. Gierada DS, Curtin JJ, Erickson SJ, Prost RW, Strandt JA, Goodman LR. Diaphragmatic motion: Fast gradient-recalled-echo MR imaging in healthy subjects. Radiology 1995;194:879-84.
8. Koo CW, Johnson TF, Gierada DS, White DB, Blackmon S, Matsumoto JM, *et al*. The breadth of the diaphragm: Updates in embryogenesis and role of imaging. Br J Radiol 2018;91:20170600.
9. Mehollin-Ray AR, Cassady CI, Cass DL, Olutoye OO. Fetal MR imaging of congenital diaphragmatic hernia. Radiographics 2012;32:1067-84.
10. Kilian AK, Schaible T, Hofmann V, Brade J, Neff KW, Büsing KA. Congenital diaphragmatic hernia: Predictive value of MRI relative lung-to-head ratio compared with MRI fetal lung volume and sonographic lung-to-head ratio. AJR Am J Roentgenol 2009;192:153-8.
11. Hammer MM, Raptis DA, Mellnick VM, Bhalla S, Raptis CA. Traumatic injuries of the diaphragm: Overview of imaging findings and diagnosis. Abdom Radiol (NY) 2017;42:1020-7.
12. Gaeta M, Musumeci O, Mondello S, Ruggeri P, Montagnese F, Cucinotta M, *et al*. Clinical and pathophysiological clues of respiratory dysfunction in late-onset pompe disease: New insights from a comparative study by MRI and respiratory function assessment. Neuromuscul Disord 2015;25:852-8.
13. Gaeta M, Barca E, Ruggeri P, Minutoli F, Rodolico C, Mazziotti S, *et al*. Late-onset pompe disease (LOPD): Correlations between respiratory muscles CT and MRI features and pulmonary function. Mol Genet Metab 2013;110:290-6.
14. Baldes N, Schirren J. Primary and secondary tumors of the diaphragm. Thorac Cardiovasc Surg 2016;64:641-6.
15. Pedrosa I, Saíz A, Arrazola J, Ferreirós J, Pedrosa CS. Hydatid disease: Radiologic and pathologic features and complications. Radiographics 2000;20:795-817.
16. Cicero G, Blandino A, Ascenti G, D'Angelo T, Frosina L, Visalli C, *et al*. Superinfection of a dead hepatic echinococcal cyst with a cutaneous fistulization. Case Rep Radiol 2017;2017:5.
17. Mazziotti S, Gaeta M, Blandino A, Barone M, Salamone I. Hepatobronchial fistula due to transphrenic migration of hepatic echinococcosis: MR demonstration. Abdom Imaging 2000;25:497-9.

How to cite this article: Cicero G, Mazziotti S, Blandino A, Granata F, Gaeta M. Magnetic resonance imaging of the diaphragm: From normal to pathologic findings. J Clin Imaging Sci 2020;10:1.

Video 1: Movie loop of magnetic resonance imaging fluoroscopy scans acquired during normal breathing and showing physiologic diaphragmatic movements.

Video 2: Polymyositis involving diaphragm. Magnetic resonance imaging fluoroscopies acquired during normal breathing respectively at the time of diagnosis (a) and after 3 months of corticosteroid therapy (b).

Video 3: Fluoroscopy magnetic resonance imaging demonstrates a severe reduction of the diaphragmatic movements due to weakness. The final diagnosis was myasthenia presenting with respiratory failure.